Secondary Structure Effect of Polypeptide on Reverse Thermal Gelation and Degradation of L/DL-Poly(alanine)–Poloxamer–L/DL-Poly(alanine) Copolymers

Hye Jin Oh, Min Kyung Joo, Youn Soo Sohn, and Byeongmoon Jeong*

Department of Chemistry, Division of Nano Sciences, Ewha Womans University, Daehyun-Dong, Seodaemun-Ku, Seoul 120-750, Korea

Received June 30, 2008; Revised Manuscript Received September 9, 2008

ABSTRACT: Poly(alanine) end-capped poly(propylene glycol)−poly(ethylene glycol)−poly(propylene glycol) (PA−PLX−PA) aqueous solutions underwent sol-to-gel transition as the temperature increased. On the basis of FTIR spectra, circular dichroism spectra, ^{13}C NMR spectra, transmission electron microscopic images, fluorescence spectra, and dynamic light scattering studies, increases in the β-sheet conformation of the polyalanine (PA) and dehydration of the poly(propylene glycol)−poly(ethylene glycol)−poly(propylene glycol) (PLX) were suggested as the sol-to-gel transition mechanism. The sol-to-gel transition temperature could be controlled by molecular parameters of the PA−PLX−PA such as molecular weight of PA, molecular weights of PLX, and L-Ala/DL-Ala ratio. The PA−PLX−PA was significantly degraded in the subcutaneous layer of rats over 15 days; however, it was stable in phosphate buffer saline over the same period of time. Poly(propylene glycol)/poly(ethylene glycol) block copolymers suffer from short gel duration for biomedical applications, whereas the current polypeptide-based polymer is unique in that it shows prolonged (>15 days) gel duration and the sol-to-gel transition involves the secondary structural change of the polypeptide.

Introduction

Reverse thermal gelation has been an important topic during the past decade not only for the unique sol-to-gel phase transition mechanism but also for the potential biomedical applications.[1,2] Without physical surgery, drug delivery depots or tissue engineering scaffolds can be prepared by the conventional syringe injection of a polymer aqueous solution containing drugs or cells. Micellar packing/aggregation, phase mixing between polymer blocks, and intermolecular bridge formation, etc., have been suggested as the mechanism of the reverse thermal gelation.[3−6] For a polymer aqueous solution to show reverse thermal gelation behavior, the polymer should have a delicate balance between hydrophilicity and hydrophobicity. Poly(propylene oxide), poly(butylenes oxide), poly(lactide-*co*-glycolide), polycarbonates, polyphosphazenes, polysaccharides, etc., have been used for the hydrophobic block, and poly(ethylene glycol)s have been most widely used for the hydrophilic block.[7−12]

Recently, polypeptide-based biomaterials have drawn attention due to (1) their well-defined secondary structural motifs such as α-helixes, β-sheets, and random coils, (2) facile control of hydrophilic/hydrophobic balance by combining various amino acids, and (3) their potential as a biocompatible material.[13−16] However, the reverse thermal gelling systems based on the synthetic polypeptide are rather limited except for a de Novo designed hairpin polypeptide (MAX).[17,18]

Here, we are reporting a reverse thermal gelation of the poly(alanine) end-capped poly(propylene glycol)−poly(ethylene glycol)−poly(propylene glycol) (PA−PLX−PA). The mechanism of sol-to-gel transition was investigated using various instrumental methods including FTIR spectroscopy, circular dichroism spectroscopy, ^{13}C NMR spectroscopy, transmission electron microscopy, fluorescence spectroscopy, and dynamic light scattering. The structure−property relationship of the sol-to-gel transition of the PA−PLX−PA aqueous solutions was investigated by varying PA length, PLX length, and L-Ala/DL-Ala ratio. The degradation of the PA−PLX−PA was investigated under in vitro (phosphate buffer saline) and in vivo (subcutaneous layer of rats) conditions.

* Corresponding author. E-mail: bjeong@ewha.ac.kr.

Experimental Section

Materials. Poly(propylene glycol)−poly(ethylene glycol)−poly(propylene glycol) bis(2-aminopropyl ether) (PLX) (M_n = 600 or 900 Da) (Aldrich) was used as received. The numbers of propylene glycol and ethylene glycol units were 3.5 and 8.5 for PLX with the molecular weight of 600 and 3.5 and 15.5 for PLX with the molecular weight of 900, respectively. *N*-Carboxy anhydrides of L-alanine, *N*-carboxy anhydrides of DL-alanine (M&H Laboratory, Korea), and 2-anilinonaphthalene (TCI) were used as received. Toluene was dried over sodium before use.

Synthesis. The PA−PLX−PA (PII) was prepared by ring-opening polymerization of the *N*-carboxy anhydrides of alanine in the presence of PLX.[19,20] PLX (3.0 g, 5.0 mmol; MW 600 Da; Aldrich) was dissolved in toluene (50 mL), and the residual water was removed by azeotropic distillation to a final volume of about 5 mL. Anhydrous chloroform/dimethyl formide (30 mL; 2/1 v/v), *N*-carboxy anhydrides of L-alanine (3.0 g, 26.0 mmol), and *N*-carboxy anhydrides of DL-alanine (3.0 g, 26.0 mmol) were added to the reaction mixtures. They were stirred at 40 °C for 24 h. The polymer was purified by repeated dissolution in the chloroform, followed by precipitation into diethyl ether (three times). The yield was 65%. Other polymers with different composition and block length were similarly prepared. Table 1 summarizes the list of polymers studied in this paper.

^{1}H and ^{13}C NMR Spectra. ^{1}H NMR spectra in CF_3COOD (500 MHz NMR spectrometer; Varian) were used to determine the composition of the polymer. ^{13}C NMR spectral changes of the PA−PLX−PA (PII; 6.0 wt % in D_2O) were investigated as a function of temperature. The solution temperature was equilibrated for 20 min at each temperature.

Gel Permeation Chromatography. The gel permeation chromatography system (Waters 515) with a refractive index detector (Waters 410) was used to obtain the molecular weights and molecular weight distributions of the polymers. *N,N*-Dimethylformamide was used as an eluting solvent. The poly(ethylene glycol)s in a molecular weight range of 400−20 000 Da were used as the molecular weight standards. An OHPAK SB-803QH column (Shodex) was used.

10.1021/ma8014504 CCC: $40.75
Published on Web 10/16/2008

Table 1. List of Polymers Studied

polymer	PA−PLX−PA[a]	L-Ala/DL-Ala[b]	M_n[c]	M_w/M_n[c]
PI	380−600−380	50/50	860	1.1
PII	430−600−430	50/50	900	1.1
PIII	530−600−530	50/50	1260	1.1
PIV	450−900−450	50/50	1050	1.1
PV	440−600−440	60/40	930	1.1
PVI	450−600−450	40/60	960	1.1
PVII	400−600−400	0/100	830	1.1
PVIII	450−600−450	100/0	850	1.1

[a] Determined by ^{1}H NMR in CF_3COOD. Structure of PA−PLX−PA: $H_2N-(CH(CH_3)CONH)_x-CH(CH_3)CH_2-(O-CH(CH_3)CH_2)_l-(OCH_2CH_2)_m-(OCH_2CH(CH_3))_n-(NHCOCH(CH_3)x\text{-}NH_2$. $l + n = 3.5$. $m = 8.5$ and 15.5 for PLX 600 and 900, respectively. Therefore, $A_{1.0-2.0}/A_{3.0-4.2} = (13.5 + 6x)/47.5$ for PLX ($M_n = 600$) and $A_{1.0-2.0}/A_{3.0-4.2} = (13.5 + 6x)/75.5$ for PLX ($M_n = 900$). x is the number of alanine repeating units of PA. $A_{1.0-2.0}$ and $A_{3.0-4.2}$ are the integration of the peaks at 1.0−2.0 and 3.0−4.2 ppm, respectively. [b] The reactivities of *N*-carboxy anhydride of L-alanine and *N*-carboxy anhydride of DL-alanine were assumed to be the same. Therefore, the feed ratio of *N*-carboxy anhydrides of L-alanine to *N*-carboxy anhydrides of DL-alanine was assumed to be the same as the ratio of L-Ala to DL-Ala of the PA−PLX−PA. [c] Determined by gel permeation chromatography using *N,N*-dimethylformamide as an eluting solvent. Poly(ethylene glycol)s were used as the molecular weight standards.

Phase Diagram. The sol−gel transition of the polymer aqueous solution was investigated by the test tube inverting method.[21,22] The aqueous polymer solution (0.5 mL) was put in the test tube with an inner diameter of 11 mm. The transition temperature was determined by the flow (sol)−nonflow (gel) criterion by an increment of 1 °C per step. Each data point is an average of three measurements.

Dynamic Mechanical Analysis. Changes in storage modulus of the polymer aqueous solutions were investigated by dynamic rheometry (Rheometer RS 1; Thermo Haake).[23] The aqueous polymer solution was placed between parallel plates of 25 mm diameter and a gap of 0.5 mm. During the dynamic mechanical analysis, the samples were located inside of a chamber with water-soaked cotton to minimize the water evaporation. The data were collected under a controlled stress (4.0 dyn/cm^2) and a frequency of 1.0 rad/s. The heating rate was 0.5 °C/min.

FTIR Spectra. IR spectra (FTIR spectrophotometer FTS-800; Varian) of the PA−PLX−PA (PII) aqueous solution (6.0 wt % in D_2O) were investigated as a function of temperature in a range of 10−60 °C with an increment of 5 °C each step. The aqueous solution was equilibrated for 20 min at each temperature.

Circular Dichroism Spectroscopy. Ellipticity of the PA−PLX−PA (PII) aqueous solution (0.05 wt %) was obtained by a circular dichroism instrument (J-810; JASCO) as a function of temperature in a range of 10−60 °C with an increment of 5 °C each step. The aqueous solution was equilibrated for 20 min at each temperature.

Critical Micelle Concentration. Critcal micelle concentration of PA−PLX−PA (PII) was investigated by fluorescence spectroscopy (RF5301; Shimadzu) at 15 °C. A 2-anilinonaphthalene solution in methanol (30 μL at 0.01 mM) was injected into a polymer aqueous solution (3.0 mL) in a polymer concentration range of 5.0×10^{-5}−5.0×10^{-1} wt %. The excitation wavelength was 309 nm. The fluorescence spectra of the solutions were recorded from 350 to 600 nm. The band position was plotted against the polymer concentration, and the crossing point of the two extrapolated lines was defined as the critical micelle concentration.[10,24]

Transmission Electron Microscopy. PA−PLX−PA (PII) aqueous solutions (0.05 wt %) were kept for 20 min at 15 and 35 °C, respectively. The PA−PLX−PA (PII) aqueous solution (10 μL) was placed on the carbon grid, and the excess solution was blotted with filter paper. The grids were dried at 15 and 35 °C for 24 h. The microscopic image was obtained by JEM-2100F (JEOL) with an accelerating voltage of 200 kV. Phosphotungstanate was used as a staining agent.

Dynamic Light Scattering. The apparent size of PA−PLX−PA (PII) aggregates in water (2.0 wt %) was studied by a dynamic light scattering instrument (ALV 5000-60x0) as a function of temperature. A YAG DPSS-200 laser (Langen, Germany) operating at 532 nm was used as a light source. Measurements of scattered light were made at an angle of 90° to the incident beam. The results of dynamic light scattering were analyzed by the regularized CONTIN method. The decay rate distributions were transformed to an apparent diffusion coefficient. From the diffusion coefficient, the apparent hydrodynamic size of a polymer aggregate can be obtained by the Stokes−Einstein equation.

Degradation of the in-Situ Formed Gel. PA−PLX−PA (PII) aqueous solutions (10.0 wt %, 0.5 mL/rat) were subcutaneously injected using a 21-gauge needle into healthy rats with a body weight of about 250 g/rat. After taking the sample at a given time interval, each rat was sacrificed. For in vitro study, the gel was formed by injecting the same PA−PLX−PA (PII) aqueous solution (0.5 mL) into a vial (inner diameter = 1.1 cm) at 37 °C, and phosphate buffer saline (3.0 mL) at 37 °C was added on the in situ formed gel. The vial was shaken with strokes 60 per minute. The buffer at 37 °C was replaced every day.

Enzymatic Degradation of the PA−PLX−PA. In vitro degradation of the PA−PLX−PA (1.0 wt % in each medium (1.0 mL)) in duplicate was studied over 72 h in phosphate buffer saline (150 mM) at pH = 7.4 for the control experiment and chymotrypsin; in phosphate buffer saline (150 mM) with 1.0 mM $CaCl_2$ at pH = 7.4 for collagenase and elastase; in phosphate buffer saline (150 mM) with 0.02 wt % Triton X-100, 0.1 mM ethylenediamine tetraacetic acid, and 5 mM glutathione at pH = 5.5 for cathepsin B.[25−29] The concentration of enzyme was fixed at 5.0 units/mL.

Results and Discussion

PA−PLX−PA was prepared by the ring open-polymerization of the *N*-carboxy anhydrides of alanine on the PLX with amino groups at the ends of the polymer. Peak areas at 3.0−4.2 ppm ($A_{3.0-4.2}$) and 1.0−2.0 ppm ($A_{1.0-2.0}$) in the ^{1}H NMR (CF_3COOD) were used to calculate the number-average molecular weight of each block of PA−PLX−PA (Supporting Information: Figure S1-a). $A_{3.0-4.2}$ is the integration area of PLX peak adjacent to oxygen or amine, that is, (OCH_2CH_2O), ($OCH_2CH(CH_3)O$), and ($OCH_2CH(CH_3)N$). $A_{1.0-2.0}$ is the integration area of methyl peak of PLX and PA, that is, ($OCH_2CH(CH_3)O$), ($OCH_2CH(CH_3)N$), and ($OCCH(CH_3)NH$). Based on the above information, $A_{1.0-2.0}/A_{3.0-4.2} = (13.5 + 6x)/47.5$ for PLX ($M_n = 600$) and $A_{1.0-2.0}/A_{3.0-4.2} = (13.5 + 6x)/75.5$ for PLX ($M_n = 900$). x is the number of alanine repeating units of PA.

To study the structure−property relationship, PA length, PLX length, and L-Ala/DL-Ala ratio were varied. Table 1 summarizes the list of polymers studied in this paper. The unimodal distribution of all the polymers in the GPC chromatograms suggests the absence of pure polypeptides, and they are purified enough to discuss the structure−property relationship (Supporting Information: Figure S1-b).

First, the molecular weight of PA was varied from 380 to 530 Da at a fixed ratio of L-Ala/DL-Ala (50/50 by mole) and the molecular weight of PLX at 600 (PI, PII, and PIII). Second, the molecular weight of PLX was varied from 600 to 900 at a fixed L-Ala/DL-Ala ratio (50/50 by mole) and the molecular weight of PA (PII and PIV). Third, L-Ala/DL-Ala was varied from 60/40, 50/50, 40/60, and 0/100 by mole at a fixed molecular weight of PA and PLX (PII, PV, PVI, and PVII). PVII consisting of DL-PA was soluble and did not show sol−gel transition in a temperature range of 0−80 °C due to its highly hydrophilic nature. PVIII with a similar molecular weight of L-PA was partially soluble in water.

The solution behavior of the PA−PLX−PA was intensively studied for PII because the polymer showed excellent reverse thermal gelling behavior in a physiologically important temperature range of 10−40 °C. PII has an L-Ala/DL-Ala ratio of 50/50 (by mole), a molecular weight of each block of 430−600−430, and a narrow molecular weight distribution of

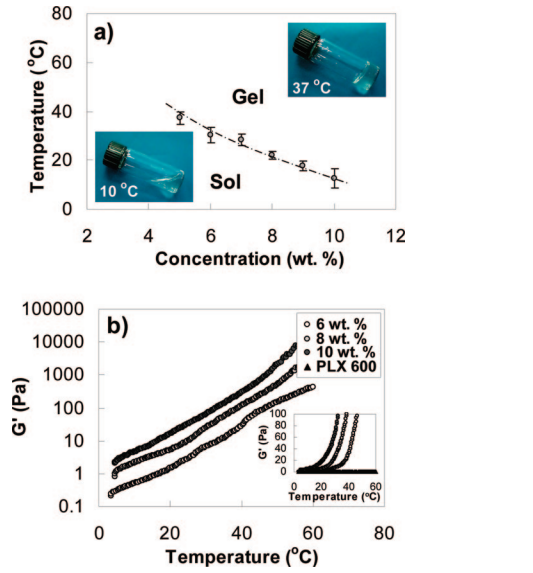

Figure 1. (a) Phase diagram of the PA−PLX−PA (PII) aqueous solutions determined by the test tube inverting method. The photos of PA−PLX−PA (PII) aqueous solutions (6.0 wt %) at 10 °C (sol) and 37 °C (gel) were inserted. (b) Increases in storage modulus (G') of the PA−PLX−PA (PII) aqueous solutions during the sol-to-gel transition. The legends are concentrations of the polymer. G' of PLX aqueous solution (10.0 wt %) is also shown for comparison. The data were obtained with a heating rate of 0.5 °C min^{-1} and a frequency of 1.0 rad/s.

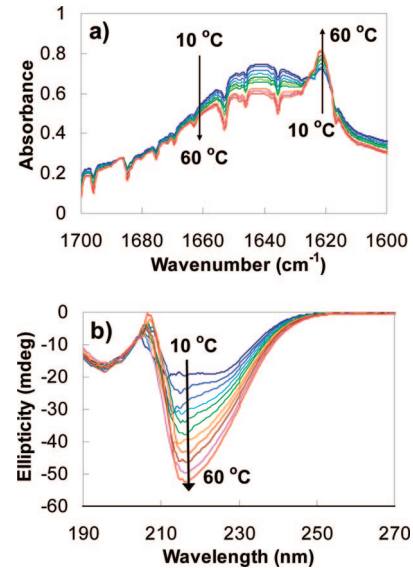

Figure 2. (a) FTIR spectra of PA−PLX−PA (PII) aqueous solution (6.0 wt %) in D_2O as a function of temperature. (b) Circular dichroism spectra of PA−PLX−PA (PII) in water (0.05 wt %) as a function of temperature. Both FTIR and circular dichroism spectra were obtained by an increment of 5 °C.

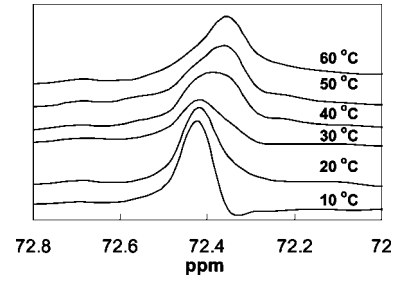

Figure 3. ^{13}C NMR spectra of the PA−PLX−PA (PII) in D_2O (6.0 wt %) as a function of temperature.

1.1. As the temperature increased, PA−PLX−PA (PII) aqueous solutions underwent sol-to-gel transition. The transition temperature decreased from 39 to 13 °C as the polymer concentration increased from 5.0 to 10.0 wt % (Figure 1a). Poloxamer (F-127: a typical reverse thermogelling poly(ethylene glycol)/poly(propylene glycol) block copolymer) has a critical gel concentration of 20−35 wt % in water;[7] however, the PA−PLX−PA showed a lower critical gelation concentration of 5.0 wt %. At concentrations higher than 11.0 wt % the PA−PLX−PA (PII) aqueous solutions remained as a gel state in a temperature range of 0−80 °C. At concentrations lower than 4.0 wt %, an increase in viscosity was observed as the temperature increased; however, the mass flow occurred in this temperature range due to the low strength of the polymer aqueous system. Photos of sol (10 °C) and gel (37 °C) states prepared from 6.0 wt % PA−PLX−PA (PII) aqueous solution are inserted in Figure 1a. At 10 °C, the polymer solution is in a free-flowing sol state; however, it turns into a gel state at 37 °C. An abrupt increase in the gel modulus was observed in the dynamic mechanical analysis as the temperature increased due to the sol-to-gel transition of the PA−PLX−PA aqueous solution (Figure 1b).[23,30,31] The frequency and the heating rate were 1.0 rad/s and 0.5 °C/min., respectively. The sol-to-gel transition temperatures determined by the test tube inverting method were well-correlated to the temperatures that the modulus began to increase abruptly.

The conformational change in PA−PLX−PA was investigated by FTIR and circular dichroism spectra as a function of temperature. A sharp band at 1624 cm^{-1}, a sharp band at 1653 cm^{-1}, and a broad band around 1640 cm^{-1} in the FTIR spectra represent β-sheet, α-helix, and random coil structures of polypeptides, respectively.[32,33] A positive Cotton band at 195 nm and a negative Cotton band at 210−220 nm; a positive Cotton band at 195 nm and two negative Cotton bands at 205−210 and 215−225 nm; and a negative Cotton band at 195 nm and a positive Cotton band at 215 nm represent β-sheet, α-helix, and random coil structures of polypeptides, respectively.[34,35] The FTIR spectra of PA−PLX−PA (PII; 6.0 wt % in D_2O) were investigated in D_2O to avoid the interruption by the O−H bending band of H_2O around 1600−1700 cm^{-1}. As the temperature increased from 10 to 60 °C, the absorption band at 1620 cm^{-1} (amide I band related to β-sheet structure) increased, whereas the broad band around 1640 cm^{-1} (amide I band related to random coil structure) decreased (Figure 2a).[32,33] Circular dichorism spectra of PA−PLX−PA (PII) aqueous solution (0.05 wt % in H_2O) also supported the change in the polypeptide conformation from random coils to β-sheets as the temperature increased. The negative band at 218 nm significantly increased in its magnitude as the temperature increased from 10 to 60 °C (Figure 2b). The negative band at 218 nm is a measure of a β-sheet structure of a polypeptide.[34,35]

A peak at 72.2−72.6 ppm of the ^{13}C NMR spectra of PA−PLX−PA (PII) aqueous solution (6.0 wt % in D_2O) showed a significant broadening as the temperature increased from 20 to 40 °C in which the sol-to-gel transition of the PA−PLX−PA aqueous solution occurred (Figure 3). The broadening of the NMR peak is an indication of a decrease in the molecular motion of the PLX that has been claimed for the dehydration of the block.[4,21,23] On the basis of the above observation, we can conclude that the dehydration of the PLX as well as the conformational change in polypeptide from random coils to β-sheets plays a critical role in the sol-to-gel transition of the PA−PLX−PA aqueous solution.

The PA−PLX−PA formed micelles in water. The fluorescence emission wavelength of 2-anilinonaphthalene is sensitive to the microenvironment, and the blue shift in the emission band

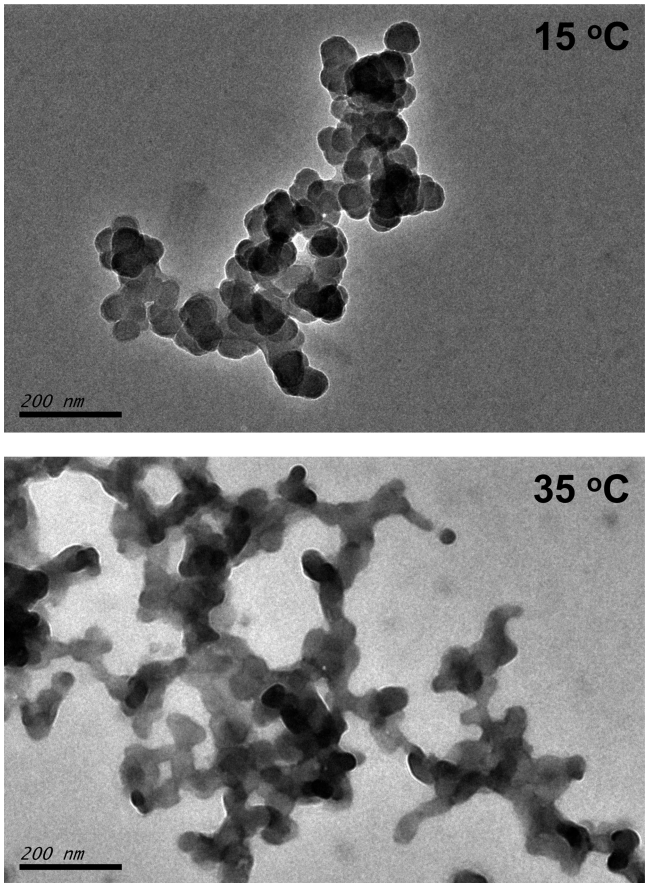

Figure 4. Transmission electron microscopic image of the PA−PLX−PA (PII). Polymer aqueous solutions (0.05 wt %) were equilibrated at 15 and 35 °C for 20 min and air-dried at each temperature. The scale bar is 200 nm.

was used for the determination of the critical micelle concentration of the polymer in water.[10,24] The critical micelle concentration of the PA−PLX−PA (PII) determined by this method was about 0.01 wt % (Supporting Information: Figure S2). The transmission electron microscopic image of the polymer developed in water at 15 °C showed spherical micellar assemblies of PA−PLX−PA (PII), whereas, the image developed at 35 °C showed cylindrical extension of the assembled polymer and spherical micelles as well (Figure 4). The transition from spherical micelles to cylindrical micelles might be cooperatively driven by the dehydration of PLX blocks[36,37] and conformational changes from random coils to β-sheets of PA blocks as the temperature increased.

Dynamic light scattering study showed the increase in the size of polymer assemblies as the temperature increased. The most probable apparent size of polymer assemblies was 40 nm at 10−20 °C, which was similar in size to the images observed by transmission electron microscopy at 15 °C. The increase in the apparent size to 100−400 nm accompanying a broad distribution of the sizes was observed as the temperature increased from 10 to 50 °C (Figure 5). This observation suggests the aggregation of the micelles or changes in the aggregation pattern that can be correlated with the transmission electron microscopic images developed at 35 °C.

The structure−property relationship of the sol−gel transition was investigated. As the PA block length increased at a fixed PLX length, the sol-to-gel transition temperature decreased (Figure 6a). As the hydrophilic PLX length increased at a similar PA length, the sol-to-gel transition temperature increased due to the increase in hydrophilicity (Figure 6b). In addition, the sol-to-gel transition temperature decreased as the L-Ala/DL-Ala

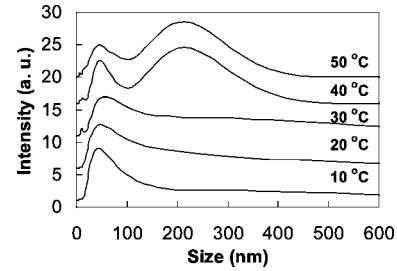

Figure 5. Apparent size distribution of the PA−PLX−PA (PII) as a function of temperature in water (2.0 wt %).

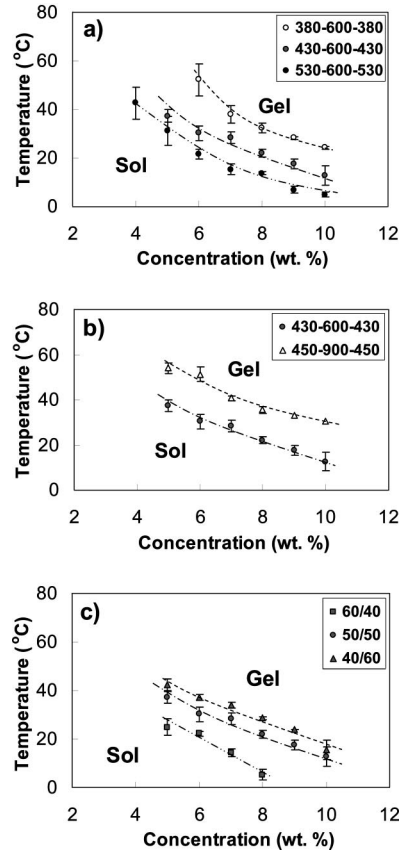

Figure 6. Phase diagram of the PA−PLX−PA aqueous solutions: (a) effect of PA molecular weight, (b) effect of PLX molecular weight, (c) effect of L-Ala/DL-Ala of PA. Transition temperatures were determined by the test tube inverting method ($n = 3$). The composition of L-Ala/DL-Ala was 50/50 (by mole) for (a) and (b). The legends in (a) and (b) are the molecular weight of each block of PA−PLX−PA. The ratio of L-Ala to DL-Ala (by mole) is shown as a legend in (c).

ratio increased (Figure 6c). The above observations suggest that PA blocks behave like hydrophobic blocks in the polyester or polycarbonate systems in the sol-to-gel transition, and the L-Ala-rich PA block is particularly effective for the gelation.[4,21,23] As the L-Ala/DL-Ala increased from 0/100 to 60/40, a characteristic β-sheet band in FTIR of the PA−PLX−PA aqueous solutions (6.0 wt % in D_2O) at 1620−1630 cm^{-1} increased (Supporting Information: Figure S3). Therefore, the PA−PLX−PA rich in L-Ala tends to more effectively form β-sheet than the polymer rich in DL-Ala, suggesting that the preassembled β-sheet structures facilitate the sol-to-gel transition.[17]

On the basis of the above observation, a sol−gel transition model can be suggested as follows. The polymer forms micelles as proven in fluorescence spectroscopy, transmission electron microscopy, and dynamic light scattering. PA blocks form a core and PLX blocks form a shell of the micelle. The PA blocks

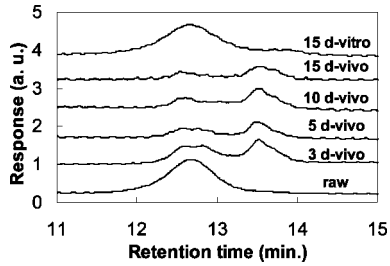

Figure 7. Gel permeation chromatograms of the PA−PLX−PA (PII) after implantation of the aqueous solution (10.0 wt %) in the subcutaneous layer of rats. The chromatogram of the PA−PLX−PA (PII) incubated in the phosphate buffer saline (15 d-vitro) for 15 days was compared.

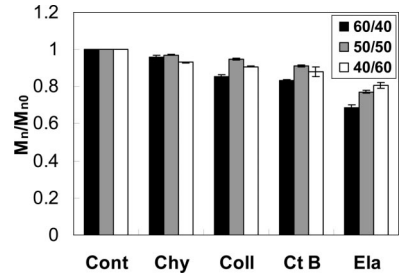

Figure 8. Enzymatic degradability of the PA−PLX−PA (PII). Cont, Chy, Coll, Ct B, and Ela stand for control (phosphate buffer saline), chymotrypsin, collagenase, cathepsin B, and elastase, respectively. The legends are the ratio of L-Ala/DL-Ala of the PA−PLX−PA (PII).

undergo a random coil-to-β-sheet transition as the temperature increases. The spherical micelles uniaxially grow to cylindrical shape as shown in transmission electron microscopic images. On the other hand, the PLX is dehydrates as the temperature increases.

The cooperative transition of PA and PLX of the PA−PLX−PA drives the sol-to-gel transition of the PA−PLX−PA aqueous solution as the temperature increased. The β-sheet extension model for sol-to-gel transition of PA−PLX−PA is clearly distinguished from the spherical micellar packing model of the poly(ethylene glycol)/poly(propylene glycol) block copolymer systems or micellar aggregation/phase mixing model of polyester-based systems.[3−6] The difference in sol-to-gel transition mechanism between PA−PLX−PA and PLX makes the PA−PLX−PA thermogel a sustainable gel with a significantly longer duration. The short gel duration has been a concern of the poly(ethylene glycol)/poly(propylene glycol) block copolymer systems for biomedical applications such as drug delivery and tissue engineering.[38] Because the PLXs of the current study did not show reverse thermal gelation in the range of 0−80 wt % and 0−80 °C, the F-127 (which has the highest gelling properties among poly(ethylene glycol)/poly(propylene glycol) block copolymers) thermogel was compared. The 3.0 mL phosphate buffer saline (150 mM) was added on top of the in situ formed gel (0.5 mL) in a shaking bath with 60 strokes/min at 37 °C. The buffer was replaced every day to mimic a sink condition. The in vitro erosion test showed that the PA−PLX−PA (prepared from 10 wt % aqueous solution) eroded less than 30 wt % in 1 month, whereas the F-127 gel (prepared from 30 wt % aqueous solution) completely disappeared less than 5 days (Supporting Information: Figure S4). The relatively stronger resistance against erosion clearly demonstrated the significance of polypeptide in stabilizing the hydrogel.

The degradation of the PA−PLX−PA (PII) was investigated by incubating the in situ formed polymer gel in the subcutaneous layer of rats as well as in phosphate buffer saline. The gel permeation chromatogram of the remaining polymer in the rat showed decrease in the molecular weight over 15 days, whereas there was no change in molecular weight when incubated in phosphate buffer saline (15 d-vitro) over the same period of time at 37 °C (Figure 7). Therefore, the decrease in the mass for in vitro erosion study (phosphate buffer saline) seems to be caused by erosion rather than hydrolysis of the PA−PLX−PA. The in vitro PA−PLX−PA degradation was studied for phosphate buffer saline (cont), chymotrypsin (Chy), collagenase (Coll), cathepsin B (Ct B), and elastase (Ela) for 72 h, as the Ala−Ala is known to be degraded by elastase.[27] The PA−PLX−PA was effectively degraded by elastase. The degradation of the PA−PLX−PA by elastase was more pronounced for the polymer with higher L-Ala content (Figure 8).

Conclusions

A reverse thermal gelling system of PA−PLX−PA was developed. As the temperature increased, changes in the secondary structure of PA from random coil-to-β-sheet and a decrease in molecular motion of the PLX were observed. The molecular weight of each block and composition of PA of PA−PLX−PA played a critical role in determining the sol-to-gel transition temperature. The PA−PLX−PA was stable in phosphate buffer saline, whereas it was significantly degraded in the subcutaneous layer of rats. The PA−PLX−PA gel significantly prolonged the gel duration of traditional poly(ethylene glycol)/poly(propylene glycol) block copolymer systems from a few days to 1 month in vivo. This paper suggests that polypeptides with a specific secondary structure provide a useful motif in designing a biomaterial with reverse thermal gelation.

Acknowledgment. This work was supported by the Korea Research Foundation (Grant KRF-2004-041-C00300) and Korea Science & Engineering Foundation (Grants R11-2005-008-00000-0 and R01-2007-000-20141-0).

Supporting Information Available: ^{1}H NMR of PLX and PA−PLX−PA, GPC chromatograms of PA−PLX−PA, determination of critical micelle concentration the PA−PLX−PA by fluorescence spectroscopy, FTIR spectra of PA−PLX−PA aqueous solutions, in vitro duration of the in situ formed PA−PLX−PA gel; photos taken 1, 3, 5, 10, 15, and 30 days after the subcutaneous injection of the PA−PLX−PA aqueous solution into rats. This material is available free of charge via the Internet http://pubs.acs.org.

References and Notes

(1) Packhaeuser, C. B.; Schnieders, J.; Oster, C. G.; Kissel, T. *Eur. J. Pharm. Biopharm.* **2004**, *58*, 445–455.
(2) Jeong, B.; Kim, S. W.; Bae, Y. H. *Adv. Drug Delivery Rev.* **2002**, *54*, 37–51.
(3) Mortensen, K.; Perdersen, J. S. *Macromolecules* **1993**, *26*, 805–812.
(4) Jeong, B.; Bae, Y. H.; Kim, S. W. *Macromolecules* **1999**, *32*, 7064–7069.
(5) Booth, C.; Attwood, A. *Macromol. Rapid Commun.* **2000**, *21*, 501–527.
(6) Fujiwara, T.; Mukose, T.; Yamaoka, T.; Yamane, H.; Sakurai, S.; Kimura, Y. *Macromol. Biosci.* **2001**, *1*, 204–208.
(7) Malmsten, M.; Lindman, B. *Macromolecules* **1992**, *25*, 5446–5450.
(8) Yang, J.; Pickard, S.; Deng, N. J.; Barlow, R. J.; Attwood, D.; Booth, C. *Macromolecules* **1994**, *27*, 2371–2379.
(9) Jeong, B.; Gutowska, A. *Trends Biotechnol.* **2002**, *20*, 305–311.
(10) Kim, S. Y.; Kim, H. J.; Lee, K. E.; Han, S. S.; Sohn, Y. S.; Jeong, B. *Macromolecules* **2007**, *40*, 5519–5525.
(11) Lee, B. H.; Lee, Y. M.; Sohn, Y. S.; Song, S. C. *Macromolecules* **2002**, *35*, 3876–3879.
(12) Chenite, A.; Chaput, C.; Wang, D.; Combes, C.; Buschmann, M. D.; Hoemann, C. D.; Leroux, J. C.; Atkinson, B. L.; Binette, F.; Selmani, A. *Biomaterials* **2000**, *21*, 2155–2161.
(13) Nowak, A. P.; Breedveld, V.; Pakstis, L.; Ozbas, B.; Pine, D. J.; Pochan, D.; Deming, T. J. *Nature (London)* **2002**, *417*, 424–428.

(14) Fairman, R.; Akerfeldt, K. S. *Curr.Opin. Struct. Biol.* **2005**, *15*, 453–463.
(15) Vandermeulen, G. W. M.; Tziatzios, C.; Duncan, R.; Klok, H. A. *Macromolecules* **2005**, *38*, 761–769.
(16) Rathore, O.; Sogah. Y. *J. Am. Chem. Soc.* **2001**, *123*, 5231–5239.
(17) Petka, W. A.; Harden, J. L.; McGrath, K. P.; Wirtz, D.; Tirrell, D. A. *Science* **1998**, *281*, 389–392.
(18) Pochan, D. J.; Schneider, J. P.; Kretsinger, J.; Ozbas, B.; Rajagopal, K.; Haines, L. *J. Am. Chem. Soc.* **2003**, *125*, 11802–11803.
(19) Lecommandoux, S.; Achard, M. F.; Langenwalter, J. F.; Klok, H. F. *Macromolecules* **2001**, *34*, 9100–9111.
(20) Jeong, Y.; Joo, M. K.; Sohn, Y. S.; Jeong, B. *Adv. Mater.* **2007**, *19*, 3947–3950.
(21) Hwang, M. J.; Suh, J. M.; Bae, Y. H.; Kim, S. W.; Jeong, B. *Biomacromolecules* **2005**, *6*, 885–890.
(22) Tanodekaew, S.; Godward, J.; Heatley, F.; Booth, C. *Macromol. Chem. Phys.* **1997**, *198*, 3385–3395.
(23) Jeong, B.; Windisch, C. F.; Park, M. J.; Sohn, Y. S.; Gutowska, A.; Char, K. *J. Phys. Chem. B* **2003**, *107*, 10032–10039.
(24) Arotcarena, M.; Heise, B.; Ishaya, S.; Laschewsky, A. *J. Am. Chem. Soc.* **2002**, *124*, 3787–3793.
(25) Soyez, H.; Schacht, E.; Vanderkerken, S. *Adv. Drug Delivery Rev.* **1996**, *21*, 81–106.
(26) Braga, P. C.; Sasso, M. D.; Culici, M.; Bianchi, T.; Bordoni, L.; Marabini, L. *Pharmacology* **2006**, *77*, 130–136.
(27) Mann, B. K.; Gobin, A. S.; Tsai, A. T.; Schmedlen, R. H.; West, J. L. *Biomaterials* **2001**, *22*, 3045–3051.
(28) Rosa, D. S.; Lopes, D. R.; Calil, M. R. *Polym. Test.* **2005**, *24*, 756–761.
(29) Kim, S.; Healy, K. E. *Biomacromolecules* **2003**, *4*, 1214–1223.
(30) Nystro1m, B.; Walderhaug, H. *J. Phys. Chem.* **1996**, *100*, 5433–5439.
(31) Chung, Y. M.; Simmons, K. L.; Gutowska, A.; Jeong, B. *Biomacromolecules* **2002**, *3*, 511–516.
(32) Ozbas, B.; Kretsinger, J.; Rajagopal, K.; Schneider, J. P.; Pochan, D. J. *Macromolecules* **2004**, *37*, 7331–7337.
(33) Rosler, A.; Klok, H. A.; Hamley, I. W.; Castelletto, V.; Mykhaylyk, O. O. *Biomacromolecules* **2003**, *4*, 859–863.
(34) Hwang, J.; Deming, T. J. *Biomacromolecules* **2001**, *2*, 17–21.
(35) Hamley, I. W.; Ansari, I. A.; Castelletto, V.; Nuhn, H.; Rosler, A.; Klok, H. A. *Biomacromolecules* **2005**, *6*, 1310–1315.
(36) Linse, P. *J. Phys. Chem.* **1993**, *97*, 13896–13902.
(37) Mao, G.; Sukumaran, S.; Beaucage, G.; Saboungi, M. L.; Thiyagarajan, P. *Macromolecules* **2001**, *34*, 552–558.
(38) Matschke, C.; Isele, U.; Hoogevest, P.; Fahr, A. *J. Controlled Release* **2002**, *85*, 1–15.

MA8014504